Journal of Applied Mechanics and Technical Physics, Vol. 50, No. 1, pp. 86–92, 2009

DIRECT SIMULATION MONTE CARLO STUDY OF THE FORMATION AND GROWTH OF CLUSTERS IN THE CASE OF VAPOR EXPANSION FROM A SUDDENLY SWITCHED SPHERICAL SOURCE

N. Yu. Bykov, G. A. Lukyanov,* and O. I. Simakova

UDC 533.6.011

The processes of formation of silicon clusters in the case of vapor expansion from a suddenly switched spherical source into an ambient inert gas are considered. Vapor expansion and condensation are described by the direct simulation Monte Carlo method. A model of clusterization is proposed, which describes reactions leading to the growth and decomposition of clusters and corresponding energy-transfer processes. The main features of cluster formation in the case of vapor expansion into a gas are considered.

Key words: *clusters, mathematical modeling, condensation, nanotechnology.*

Introduction. Studying the formation and growth of clusters in the case of vapor expansion into a gas with a low pressure is important for various applications, which include, for instance, the synthesis of clusters and cluster materials from vapor produced by intense evaporation of condensed substances [1, 2]. Of significant interest, for example, are problems of expansion and condensation of vapor formed owing to laser evaporation of small solid particles of aerosols [3, 4]. In the general case, such problems are rather complicated, because the theoretical study should involve a large number of various interrelated physical processes, including radiation absorption, heating, melting, and evaporation of matter, and expansion of the resultant vapor with allowance for clusterization processes. As such problems are extremely complicated and involve many parameters, it is difficult to study the general laws of the processes of cluster formation owing to intense expansion of vapor. In addition to solving complicated realistic problems, therefore, it is also necessary to solve appropriate problems in simpler model formulations.

The present paper describes a model formulation of the problem of cluster formation in the case of expansion of silicon vapor generated by a suddenly switched spherical source (SSS) into a buffer gas (argon) under conditions typical of pulsed laser-induced ablation of small aerosol particles. The SSS model is one of the simplest models of unsteady gas dynamics and is widely used in studying relaxation processes in pulsed jet flows [5, 6]. Until now, the possibility of a detailed study of the processes of cluster formation and growth under the conditions of intense nonequilibrium expansion of vapor has been restricted by the lack of appropriate models of cluster formation, which would adequately describe these processes as a whole (beginning from the formation of dimers) with allowance for the set of elastic and inelastic interactions of vapor particles. Some variants of such models [7–9] based on the Direct Simulation Monte Carlo (DSMC) method and including the processes of particle collisions and energy exchange between the particles, which are described with different degrees of approximation, have appeared recently. The algorithm chosen in the present work for vapor motion calculations is the variant of the DSMC method used in [7, 10] for modeling expansion of the products of laser-induced ablation of a flat target. The model of cluster formation and growth proposed in [7] was used to calculate vapor expansion into vacuum. The present paper describes a complete model of clusterization in the case of vapor expansion into a low-pressure inert ambient gas.

*Deceased.

Center for Advanced Studies at the St.-Petersburg State Polytechnical University, St. Petersburg 195251; nbykov2006@yandex.ru; vakulova@inbox.ru. Translated from Prikladnaya Mekhanika i Tekhnicheskaya Fizika, Vol. 50, No. 1, pp. 101–109, January–February, 2009. Original article submitted December 11, 2007.

Mathematical Model and Formulation of the Problem. For modeling the flow of condensing vapor, we used the DSMC algorithm with a no-time-counter collision scheme [11]. The domain of simulations is the space between the evaporating spherical surface and the outer boundary located at a sufficiently large distance from the spherical surface: $L = R_\infty - R_w$ (R_w is the sphere radius and R_∞ is the radius of the outer boundary).

The initial and boundary conditions are formulated as follows. At the initial time ($t = 0$), the domain of simulations ($r > R_w$) is filled by the background gas (argon) with a concentration n_2 and temperature T_2; there are no vapor atoms in this gas. At $t = 0$, the gas (silicon atoms) starts to evaporate from the surface ($r = R_w$). The evaporation process is described by the Hertz–Knudsen law, which implies that the flux of evaporating silicon atoms is

$$F^+ = \frac{1}{4}\, n_s u_{\rm av} = \frac{p_s(T_w)}{(2\pi m k_{\rm B} T_w)^{1/2}}.$$

Here n_s and p_s are the concentration and pressure of saturated vapor at the surface temperature T_w, $u_{\rm av} = (8k_{\rm B}T_w/(\pi m))^{1/2}$ is the mean thermal velocity of evaporating atoms, $k_{\rm B}$ is the Boltzmann constant, and m is the atomic mass. The pressure $p_s(T_w)$ is found from the Clapeyron–Clausius equation [12]. In the SSS model considered, the temperature T_w and, hence, the flux F^+ do not change with time.

For particles evaporating from the surface at $t > 0$, the velocity distribution function is assumed to be constant in time and to be semi-Maxwellian:

$$f_w^+ = \frac{F^+}{2\pi}\Big(\frac{1}{RT_w}\Big)^2 \exp\Big(-\frac{v_r^2 + v_\varphi^2 + v_\theta^2}{2RT_w}\Big) = \frac{n_s}{(2\pi RT_w)^{3/2}} \exp\Big(-\frac{v_r^2 + v_\varphi^2 + v_\theta^2}{2RT_w}\Big), \qquad v_r > 0.$$

Here v_r, v_φ, and v_θ are the components of the thermal velocity of particles and R is the gas constant. Particles returning to the source surface are excluded from the modeling process, which corresponds to the condition of their complete condensation. Particles that reach the outer boundary of the domain of simulations $r = R_\infty$ are also excluded from the calculation (supersonic output boundary).

The clusterization model implies that all particles are neutral, and clusters are formed as a result of particle collisions. The model takes into account the following processes:

1) elastic collision of atoms $A + A \longrightarrow A' + A'$;
2) recombination of atoms $A + A + A \longrightarrow A_2' + A'$;
3) association of a cluster and an atom $A_i + A \longrightarrow A_k'$ $(k = i + 1)$;
4) association of clusters $A_i + A_j \longrightarrow A_k'$ $(k = i + j)$;
5) evaporation of a monomer from a cluster $A_k \longrightarrow A_{k-1}' + A'$.

Here the primed quantities refer to particles after the collision; A stands for a silicon atom.

If there is also a buffer gas, the following reactions have to be taken into account:

— elastic collision of atoms of a buffer gas $B + B \longrightarrow B' + B'$;
— elastic collision of silicon atoms and buffer-gas atoms $A + B \longrightarrow A' + B'$;
— three-particle recombination $A + A + B \longrightarrow A_2' + B'$;
— elastic collision of clusters and buffer-gas atoms $A_k + B \longrightarrow A_k' + B'$.

Here B stands for a buffer-gas atom.

Particle collisions are described by the hard sphere model. The parameters of the cluster A_k are the number of atoms k, mass m_k, radius r_k, translational velocity $\boldsymbol{v}_k$, internal energy $E_{{\rm int},k}$, and binding energy $E_b(k)$. In accordance with the liquid spherical drop model [1], the cluster radius is determined by the formula

$$r_k = r_w k^{1/3}, \qquad r_w = (3m/(4\pi\rho))^{1/3},$$

where r_w is the Wigner–Seitz radius and ρ is the density of the cluster-forming material.

The model considered implies that clusters possess completely excited rotational and vibrational degrees of freedom. The internal energy of the cluster A_k is presented in the form

$$E_{{\rm int},k} = E_{r,k} + E_{v,k}, \qquad E_{r,k} = \zeta_r k_{\rm B} T_{r,k}/2, \qquad E_{v,k} = \zeta_v k_{\rm B} T_{v,k}.$$

Here $E_{r,k}$ and $E_{v,k}$ are the energies of rotational and vibrational degrees of freedom, ζ_r and ζ_v are the numbers of rotational and vibrational degrees of freedom, and $T_{r,k}$ and $T_{v,k}$ are the rotational and vibrational temperatures of the cluster. For a dimer, we have $\zeta_r = 2$ and $\zeta_v = 1$; for other clusters, $\zeta_r = 3$ and $\zeta_v = 3k - 6$. It is assumed that $T_{r,k} = T_{v,k} = T_{{\rm int},k}$ ($T_{{\rm int},k}$ is the internal temperature of the cluster A_k).

To determine the binding energy $E_b(k)$, we used the data [13] approximated by the formula

$$E_b(k)/k = 4.5 - 12.384 \exp(-k^{2/3})$$

(E_b is measured in electron-volts).

The model of evaporation is based on the approximate formula of the Rice–Ramsperger–Kassel theory determining the rate of decomposition of polyatomic molecules [see process (5)]. In accordance with this formula, the frequency of atom evaporation from the cluster is determined as

$$\nu = \nu_0 k_s \exp(-\zeta_v \Delta E_b / E_{v,k}), \qquad \Delta E_b = E_b(k) - E_b(k-1)$$

(ν_0 is the characteristic frequency of oscillations and k_s is the number of surface atoms). In the calculations performed, $k_s = k$ (because of the small size of the clusters obtained) and $\nu_0 = 10^{13}$ sec^{-1}.

The model of energy transfer inherent in the processes considered is based on the Larsen–Borgnakke model [11] described in detail in [7].

The following dimensionless parameters are used to analyze and present the results of simulations:

$$\frac{n}{n_s}, \quad \frac{u}{(2RT_w)^{1/2}} = \beta u, \quad \frac{T}{T_w}, \quad c_k = n_k \Big/ \sum_{k=1}^{\infty} k n_k, \quad \tau = \frac{t}{t_0}.$$

Here u is the mean flow velocity, β is a quantity inversely proportional to the most probable velocity of vapor particles, c_k is the volume fraction of the cluster A_k, and $t_0 = R_w/\sqrt{2RT_w} = \beta R_w$ is the characteristic "gas-dynamic" time.

For particular substances (in our case, silicon and argon) with a specified initial distribution function for velocities and with specified rates of reactions of cluster formation and decomposition, the examined flow (field of dimensionless parameters) is uniquely determined by the following parameters: Knudsen number Kn $= \lambda_s/R_w$ (λ_s is the mean free path of silicon atoms determined from the equilibrium concentration of vapor n_s), the dimensionless time $\tau = t/(\beta R_w)$, the ratio of concentrations of vapor and background gas n_s/n_2, and the ratio of temperatures T_w/T_2.

Results of Simulations and Analysis. The simulations were performed for a spherical source of atomic silicon vapor at $T_w = 6000$ K and Knudsen numbers Kn $= 0.01$ ($R_w = 10^{-6}$ m) and Kn $= 0.001$ ($R_w = 10^{-5}$ m). The characteristic ratio of temperatures of silicon vapor and argon was $T_w/T_2 = 20$.

First, we consider the gas-dynamic structure and flow parameters. Figure 1 shows the concentrations n/n_s, velocities βu, and temperatures T/T_w for a mixture of silicon and argon with Kn $= 0.001$, $n_2/n_s = 0.1$, and $\tau = 5$ calculated with and without allowance for condensation. Figure 1a also shows the silicon-vapor and argon concentrations in the flow with condensation.

The main laws of gas expansion into an ambient space from a suddenly switched source are known [5, 6]. The gas-dynamic structure of the flow at each particular time is determined by instantaneous positions of there characteristic gas-dynamic discontinuities (Fig. 1a): primary (bow) shock wave SW1 propagating in the ambient gas, contact surface CS separating vapor and ambient gas, and secondary shock wave SW2 formed in the course of vapor expansion. The expanding vapor plays the role of a spherical piston. In the model proposed, the contact surface CS is the layer of mixing of vapor and ambient gas. The CS position is assumed to be the radius r_k at which identical concentrations of silicon vapor and argon are reached. These discontinuities separate four regions of the flow: region of supersonic free expansion of vapor I, region of the compressed vapor layer II, region of the compressed argon layer III, and region of the undisturbed ambient gas IV (Fig. 1a). The CS radius r_k increases with time. The mass of argon displaced by vapor also increases. The momentum flux from the source remains constant. Thus, the velocity of motion of the ambient gas in region III decreases, and the shock wave SW1 decays. In region I, the gas-dynamic parameters behave in the same manner as in the case of vapor expansion from a spherical source into vacuum [6]: the density, temperature, and pressure decrease, and the velocity increases. Region I is bounded by the shock wave (SW2) at which the supersonic vapor flow becomes subsonic. In passing through this shock wave, the density, temperature, and pressure increase, and the velocity decreases.

Figure 2 shows the trajectories of motion of the shock waves SW1 and SW2 and the contact surface CS for Kn $= 0.001$ and $n_2/n_s = 0.01$, which were calculated with and without allowance for condensation. With time, the shock wave corresponding to SW1 and the contact surface monotonically move away from the source with a decreasing velocity, whereas the shock wave corresponding to SW2 reaches a steady position, which depends on the

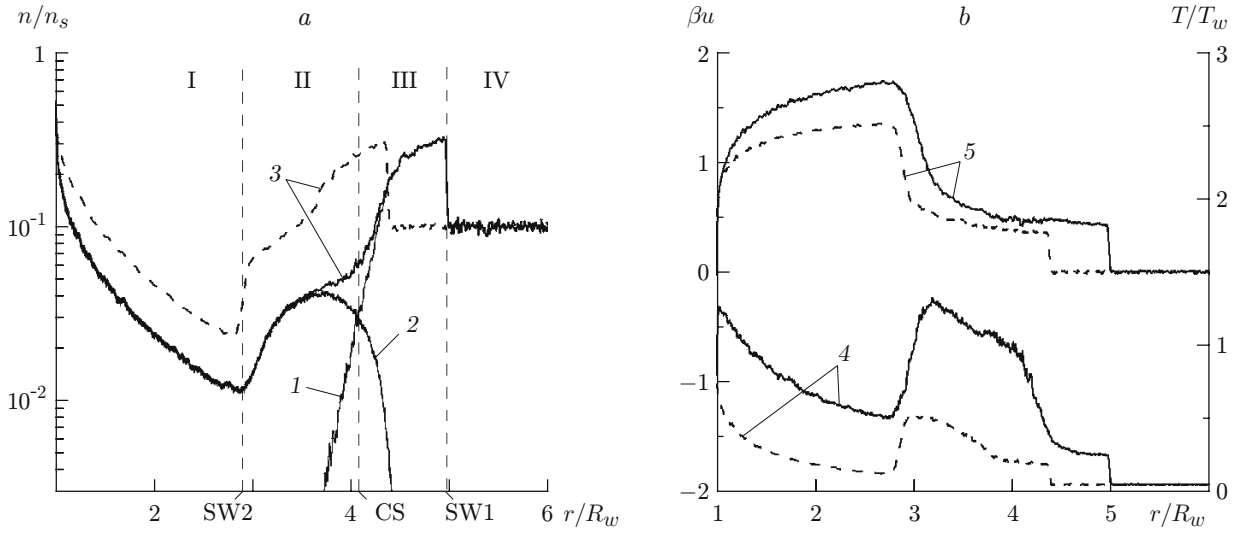

Fig. 1. Concentrations n/n_s of the mixture and individual species (a), velocities βu and temperatures T/T_w of the mixture (b) for Kn $= 0.001$, $n_2/n_s = 0.1$, and $\tau = 5$: the solid and dashed curves show the results with and without condensation in the flow, respectively; 1) concentration of argon; 2) concentration of silicon; 3) concentration of the mixture of argon and silicon; 4) velocity of the mixture of argon and silicon; 5) temperature of the mixture of argon and silicon; different regions of the flow are indicated by I–IV: region of supersonic free expansion of vapor (I), region of the compressed vapor layer (II), region of the compressed argon layer (III), and region of the undisturbed external gas (IV).

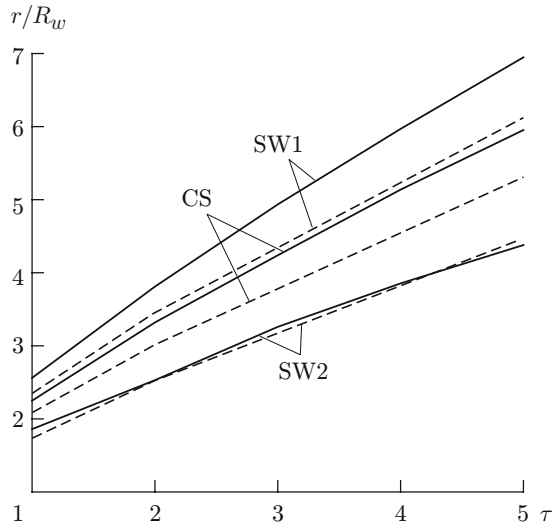

Fig. 2. Trajectories of motion of the characteristic surfaces for Kn $= 0.001$ and $n_2/n_s = 0.01$ with condensation in the flow (solid curves) and without condensation in the flow (dashed curves).

magnitude of n_2/n_s: with decreasing n_2/n_s, the limiting (steady) distance between the secondary shock wave SW2 and the source increases.

The data plotted in Figs. 1 and 2 show that vapor condensation exerts an overall strong effect on the flow structure and parameters for Kn $= 0.001$. Condensation has a rather weak effect on the size of the free expansion region I, but leads to a significant increase in the size of the compressed layer II. As a result, the size of the entire flow region increases. In region I, condensation and accompanying heat release lead to an increase in temperature (see Fig. 1b) and to a decrease in the concentration of the mixture (see Fig. 1a). The pressure in the mixture increases, which enhances the velocity of vapor expansion (see Fig. 1b). Vapor condensation with formation of

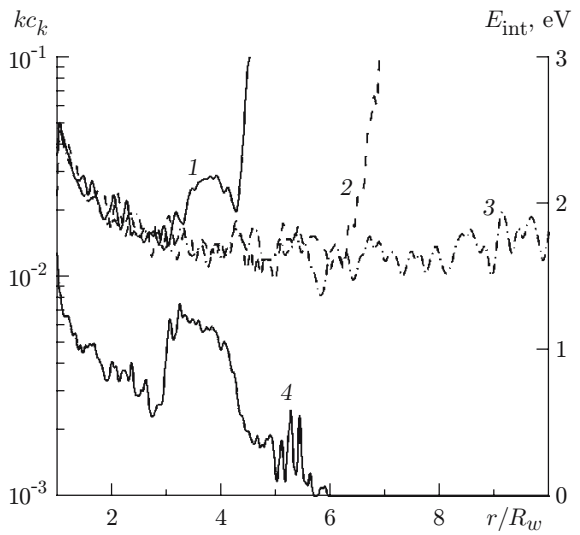

Fig. 3. Mass fraction $kc_k(r/R_w)$ of clusters A_k ($k = 2$) (curves 1–3) and their internal energy (curve 4) for Kn $= 0.001$ and $\tau = 5$: $n_2/n_s = 0.1$ (1 and 4), 0.01 (2), and 0 (3).

small clusters starts in an immediate vicinity of the source surface, where the maximum vapor density is observed. For Kn $= 0.001$, the maximum temperature $T \simeq 1.25T_w$ at $\tau > 1$ is reached at the point $r/R_w \simeq 1.1$ (in Fig. 1b, this maximum is not distinguished because of the large scale of the figure).

Strong heating of vapor during condensation leads to a significant decrease in the Mach number in region I. Ahead of the shock wave SW2, the Mach number is M ≈ 2.5 (if there is no condensation, M $\simeq 4.2$). A significant decrease in the Mach number ahead of the shock wave SW2 leads to less intense compression and heating of vapor on this wave. The total effect of condensation on flow parameters in region II is manifested in a substantial decrease in concentration and in temperature growth.

Let us consider the specific features of the parameters of the components of the mixture (atoms and clusters). Figure 3 shows the behavior of the internal energy E_{int} of the clusters A_k ($k = 2$) in the flow with $\tau = 5$, Kn $= 0.001$, and $n_2/n_s = 0.1$ (curve 4). In region I of free expansion of vapor, which is adjacent to the source surface ($r \leqslant 3R_w$), the value of E_{int} decreases, and the ambient gas exerts no effect on E_{int}. The internal energy of the clusters drastically increases in the secondary shock wave ($r/R_w \simeq 3$) and then slowly decreases in the compressed vapor layer ($r/R_w \simeq 3$–4). Further downstream, there is a compressed layer of the ambient gas (region III) whose temperature is higher than that of undisturbed argon, but substantially lower than that in the silicon cloud. Collisions with comparatively cold particles of the ambient gas lead to rapid reduction of the internal energy of the clusters.

A comparison of the distributions $kc_k(r/R_w)$ ($k = 2$) for different values of the ambient gas density (curves 1–3 in Fig. 3) shows that the mass fractions of all clusters, as well as other vapor parameters, in the region of free expansion of the silicon cloud are independent of the parameter n_2/n_s, and their distributions are similar to the distributions in the case of expansion into vacuum. The dependences $kc_k(r/R_w)$ are qualitatively identical for all cluster sizes. Both small clusters ($k = 2, 3$) and large clusters are formed near the source surface in the dense part of the free expansion region. When the maximum value is reached (this maximum cannot be distinguished in Fig. 3 because of the large scale of the figure), the values of kc_k for the clusters A_k ($k = 2$–10) in the free expansion region monotonically decrease.

The basic processes in region II containing the main mass of evaporating matter are vapor heating and compression, and also a change in the internal energy of the clusters. This fact exerts a significant effect on changes in the mass fractions of the clusters, and the behavior of kc_k is essentially different for small and large clusters. In region II, one can observe competing processes of cluster agglomeration whose intensity increases with increasing density of silicon and evaporation (the rate of evaporation substantially increases because of the jumplike growth of the cluster temperature in region II). As a result, the mass fraction of small clusters increases (see Fig. 3), and the mass fraction of large clusters decreases.

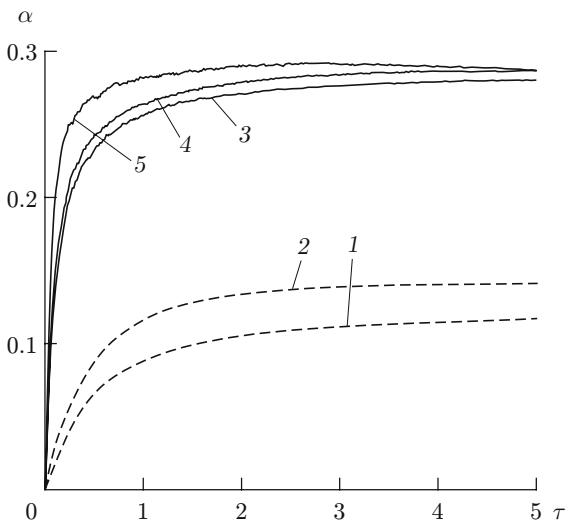

Fig. 4

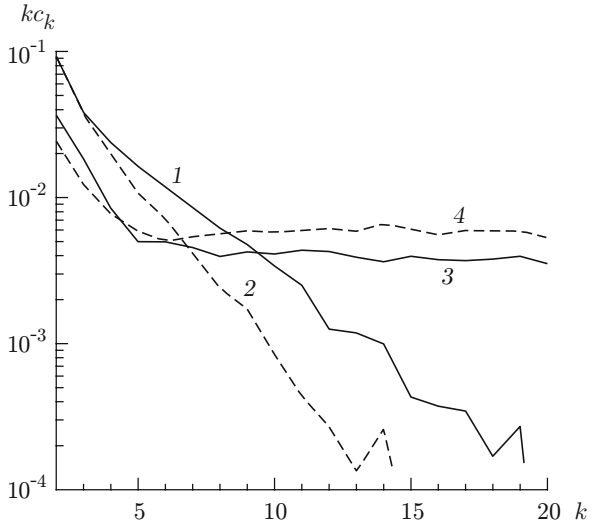

Fig. 5

Fig. 4. Total mass fraction of clusters α versus time τ: 1) Kn $= 0.01$ and $n_2/n_s = 0$; 2) Kn $= 0.01$ and $n_2/n_s = 0.1$; 3) Kn $= 0.001$ and $n_2/n_s = 0$; 4) Kn $= 0.001$ and $n_2/n_s = 0.01$; 5) Kn $= 0.001$ and $n_2/n_s = 0.1$.

Fig. 5. Dependences $kc_k(k)$ for $\tau = 5$: 1) Kn $= 0.01$ and $n_2/n_s = 0.1$; 2) Kn $= 0.01$ and $n_2/n_s = 0$; 3) Kn $= 0.001$ and $n_2/n_s = 0.1$; 4) Kn $= 0.001$ and $n_2/n_s = 0$ (4).

Region III is mainly filled by compressed argon; the argon temperature is significantly lower than the temperature of silicon vapor in region II, whereas the compressed argon concentration is much higher than the concentration of silicon vapor in region II. Only very few silicon atoms and clusters penetrate into region III. The composition of silicon vapor changes with distance from the contact surface CS in the downstream direction: the fraction of atoms decreases, and the fraction of clusters increases. As a result, the mass fraction of clusters increases (see Fig. 3), which is not a consequence of condensation; there are no collisions of silicon particles in this flow region because of the low concentration of silicon vapor.

Figure 4 shows the time evolution of the total (over the entire volume of the vapor cloud) mass fraction of clusters α for Kn $= 0.010$ and 0.001 and different densities of the ambient gas. Under conditions considered, the presence of the ambient gas exerts an insignificant effect on the total level of vapor condensation, because condensation mainly occurs in the region of free expansion of vapor and comes to an end by the time $\tau = 1$–2 owing to stabilization of a steady flow regime in the dense zone of the flow adjacent to the source. After "freezing" of the vapor composition at Kn $= 0.001$, the total level of condensation is approximately twice the value of α at Kn $= 0.01$.

The distributions of the mass fraction of clusters in terms of their size $kc_k(k)$, averaged over the cloud volume, with $\tau = 5$ and Knudsen numbers Kn $= 0.010$ and 0.001 are plotted in Fig. 5 for $n_2/n_s = 0$ and 0.1. At Kn $= 0.01$, the size of the clusters formed is rather small, and the mass fraction of clusters rapidly decreases with increasing k. The value $kc_k > 0.001$ is typical for clusters with $k < 10$–12. The presence of the ambient gas exerts practically no effect on the mass fraction of dimers and trimers, but leads to an increase in the value of kc_k for clusters with $k \geqslant 4$. At Kn $= 0.001$, the distribution $kc_k(k)$ has a different character. The mass fraction of dimers and trimers remains extremely high, and the distribution $kc_k(k)$ for clusters with $k > 4$ in the range $k = 4$–50 is close to uniform. The parameter n_2/n_s exerts only a minor effect on the distribution $kc_k(k)$. For smaller values of Kn, the distribution $kc_k(k)$ can be expected to evolve into a dependence with a maximum at a certain value $k_m \gg 1$.

The Knudsen number, which is the main criterion of similarity under conditions considered and characterizes the process of vapor condensation, can be presented as

$$\mathrm{Kn} = \frac{\lambda_s}{R_w} = \frac{1}{\sqrt{2}\, n_s \sigma_1 R_w} = \frac{k_\mathrm{B} T_w}{\sqrt{2}\, \sigma_1} \frac{1}{p_s R_w},$$

where p_s is the pressure of equilibrium silicon vapor on the source surface at $T = T_w$ and σ_1 is the collision cross section of silicon atoms. It follows from the last relation that the Knudsen number at $T_w = \mathrm{const}$ is determined by the value of $p_s R_w$. The calculated results plotted in Fig. 4 show that the total mass fraction of clusters α is proportional to Kn^{-s}, where $s < 1$ (at $\mathrm{Kn} = 0.010$–0.001, we have $s \simeq 0.3$).

The presented results of calculations of the process of cluster formation owing to laser-induced evaporation of aerosol particles ($R_w = 10^{-7}$–10^{-5} m) give a general idea about the evolution of the flow structure and parameters in the vicinity of a small particle evaporating under laser radiation and about the main features of the processes of cluster formation in such a flow. The examined model of a suddenly switched spherical source approximately simulates vapor expansion into vacuum or gas from the evaporating particle only at the initial stage of intense evaporation. Expansion of the vapor cloud formed from a single particle after its evaporation is described by another model, which takes into account the finite duration of the laser pulse. In a more detailed formulation, one has to take into account the change in the particle size, the evolution of the thermal state of the particle, and the time dependence of laser radiation intensity.

The calculations show that the influence of the ambient gas on condensation in the considered model of condensing vapor expansion into the ambient gas is insignificant. This does not mean, however, that the ambient gas does not affect condensation at all during rapid evaporation of small particles. A significant effect of the ambient gas on condensation is possible (and takes place if the ambient gas density is rather high) at the subsequent isobaric (diffusion) stage of vapor expansion into the gas.

This work was supported by the Russian Foundation for Basic Research (Grant No. 07-01-00354).

REFERENCES

1. B. M. Smirnov, "Processes in the plasma and gases with participation of clusters," *Usp. Fiz. Nauk*, **167**, No. 11, 1169–1200 (1997).
2. B. M. Smirnov, "Generation of cluster beams," *Usp. Fiz. Nauk*, **173**, No. 6, 609–648 (2003).
3. Yu. D. Kopytin, E. T. Protasevich, L. K. Chistyakova, and V. I. Shishkovskii, *Effect of Laser and Microwave Radiation on an Air Medium* [in Russian], Nauka, Novosibirsk (1992).
4. G. A. Lukyanov, Y. Khang, D. V. Leshchev, et al., "Modeling of processes of clusters formation under pulsed laser ablation of carbon particles in an aerosol," *Fullerenes, Nanotubes, Carbon Nanostruct.*, **14**, Nos. 2/3, 507–512 (2006).
5. S. F. Chekmarev, *Pulse Gas Flows in Supersonic Nozzles and Jets* [in Russian], Inst. Thermophys., Sib. Div., Acad. of Sci. of the USSR, Novosibirsk (1989).
6. G. G. Dulov and G. A. Lukyanov, *Gas-Dynamics of Expansion Processes* [in Russian], Nauka, Novosibirsk (1984).
7. N. Yu. Bykov and G. A. Lukyanov, "Direct simulation Monte Carlo of pulsed laser ablation of metals with clusterization processes in vapor," *Thermophys. Aeromech.*, **13**, No. 4, 523–536 (2006).
8. T. E. Itina, M. Sentis, and W. Marine, "Synthesis of nanoclusters by nanosecond laser ablation: Direct simulation Monte Carlo," *Appl. Surf. Sci.*, **252**, 4433–4438 (2006).
9. M. I. Zeifman, B. J. Garison, and L. V. Zhigilei, "Combined molecular dynamics — direct simulation Monte Carlo computation study of laser ablation plume evolution," *J. Appl. Phys.*, **92**, No. 4, 2181–2193 (2002).
10. N. Yu. Bykov and G. A. Lukyanov, "Modelling of pulsed laser ablation of solids on the basis of thermal model and DSMC method," *Thermophys. Aeromech.*, **10**, No. 3, 391–400 (2003).
11. G. A. Bird, *Molecular Gas Dynamics and Direct Simulation of Gas Flows*, Clarendon Press, Oxford (1994).
12. A. V. Bulgakov and N. M. Bulgakova, "Gas-dynamic effects of the interaction between a pulsed laser-ablation plume and the ambient gas: analogy with an underexpanded jet," *J. Phys. D: Appl. Phys.*, **31**, 693–703 (1998).
13. Bei Liu, Zhong-Yi Lu, Bicai Pan, et al., "Ionization of medium-sized silicon clusters and the geometries of the cations," *J. Chem. Phys.*, **109**, No. 21, 9401–9409 (1998).